

Detailed analysis of spray structure and air entrainment in GDI sprays using a tomographic approach

C. Seibel¹, K. Gartung¹, S. Arndt¹, B. Weigand²

1. Robert Bosch GmbH, 70049 Stuttgart, Germany

2. ITLR University of Stuttgart, 70569 Stuttgart, Germany

Spray characteristics of a high pressure gasoline injector are examined using experimental methods and Euler-Lagrangian spray simulation. A spray guided concept is considered where the mixture preparation is dominated by the spray dynamics and its interaction with the gas phase. To visualize the spatial distribution of the liquid phase a tomographic approach is chosen. Particular interest is given to spray-gas interaction. Therefore high resolution vector fields of the spray induced gas velocity are determined by particle image velocimetry and compared with simulation results. Air entrainment is seen as a key subject for mixture preparation as it is a rate controlling process for vaporization. An approach to quantify the air entrainment from experimental as well as simulation data is shown. All experiments are carried out in a pressure chamber at engine like ambient conditions.

1. Introduction

Gasoline direct injection is seen to have a great potential for improving the fuel economy of spark ignition engines. The main challenge is to provide an ignitable mixture in the vicinity of the spark plug under different engine conditions. Different concepts are considered to achieve these goals, wall guided, air guided and spray guided concepts [1]. Among these the later is seen as the most promising. In this configuration the spray dynamics itself dominate the mixture preparation. The spray-gas momentum transfer results in a spray induced gas velocity field which determines in conjunction with the spray dynamics the spray propagation and the distribution of the liquid and the gas phase. Furthermore the induced gas velocity field provides air entrainment into the spray [2]. The entrained air enhances the vaporization process as it supplies it with fresh air. For a successful implementation of the spray guided concept in future engines a detailed understanding of these processes is necessary.

The laser light sheet technique is a common method to determine liquid distributions in sprays, but it only provides two-dimensional information. Therefore this method is been expanded into a tomographic approach [3]. The particle image velocimetry (PIV) provides the gas velocity field in the vicinity of the spray. This information is used to calculate the air entrainment into the spray. In regions where the gas velocity field cannot be determined experimentally spray simulation can provide the missing data.

2. Experimental setup

The experimental setup for the spray tomography and PIV is shown in figure 1. The experiments are carried out in a pressure chamber at engine like pressures of up to 2 MPa

and temperatures of up to 400°C. Nitrogen is used as gas and a slight constant flow is imposed to avoid obscuration of the chamber windows. The beam of a Nd:YAG-laser (532 nm, 50 mJ, double pulsed) is separated into two equally intensive beams which are formed by a lens system to flat light sheets and guided into the chamber from both sides. A high resolution CCD camera (PCO-Sensicam) is used to record the images. For all experiments carried out in this work the rail pressure was 20 MPa, the chamber pressure 0,6 MPa and the chamber temperature 20°C. The injection duration was 1.1 ms.

For the PIV measurements alcohol particles are added as tracers which have a size of 1 to 3 μm . Double shot images with a pulse separation of 30 μs are recorded and evaluated using PIV-software (LaVision).

For spray tomography the laser, the camera and the whole optical setup are mounted on the same base plate. This plate can be moved with high precision motors to traverse the light sheet through the spray.

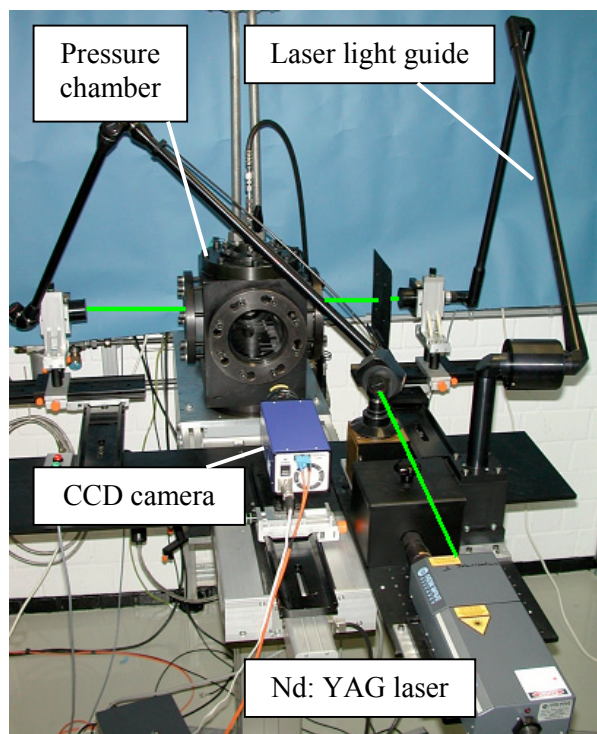


Figure 1: Experimental setup for laser light sheet technique and PIV.

3. Numerical simulation

The three dimensional spray calculations are performed using the CFD-Code FIRE. The computational model is based on the particle tracking method. According to this approach the spray droplets are described by an Lagrangian approach while the gas phase is treated in an Eulerian way. Phase coupling is achieved by source terms in the governing equations [4]. N-heptane is considered as fuel just as in the experimental investigations. The droplet start velocities and the droplet size distribution are chosen that the spray propagation is in good agreement with experimental data. No breakup model is used. The computational grid is a polar mesh with local refinement which consists of 78000 cells.

4. Results and discussion

4.1. Distribution of liquid and gas phase

For a three dimensional visualization of the liquid distribution the laser light sheet technique has been expanded into a tomographic approach. According to this approach individual light sheets are recorded traversing through the spray and interpolated to get a 3D information of the recorded Mie-intensities. Isosurfaces of constant intensity values show the overall spray shape. Arbitrary volume cuts can be generated to visualize the liquid distribution inside the spray. In figure 2 tomographic images of an annular orifice spray are shown. The volume data are based on light sheet images which are an average of 20 injections. The rugged surface after end of injection (EOI) results from shot to shot variations when the spray propagation is driven by the spray induced gas flow rather than the spray dynamics. The transient development of liquid distribution first shows a hollow cone spray. After EOI however the liquid is accumulated gradually in the center of the spray. To understand this development the spray induced gas flow has to be considered.

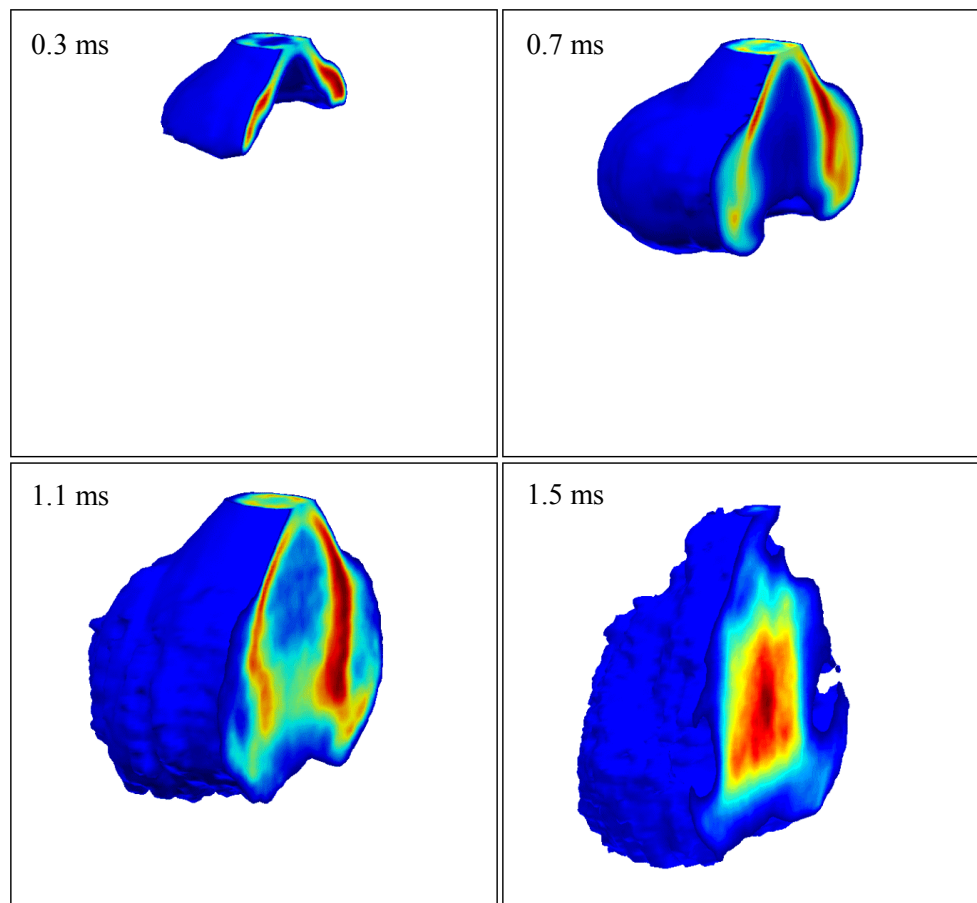


Figure 2: Tomographic images at different time steps, annular orifice spray, injection duration 1.1 ms.

4.2. Spray induced air flow

For the annular orifice injector PIV measurements of the gas flow field are shown in figure 3. The corresponding light sheets are overlaid in the images. It can be seen that an intense recirculating gas flow is induced by the spray which remains even after EOI. Small droplets,

which rapidly lose their momentum, are carried away with the gas flow and build a characteristic vortex at the head of the spray. After EOI the spray induced gas flow results in an accumulation of liquid in the center of the spray.

Due to the density of the spray no gas flow field can be obtained in the center of the spray by PIV measurements, whereas numerical simulation gives a quantitative flow field in the whole region of interest. However PIV measurements cannot be discarded as they are necessary to validate the spray simulation. In figure 4 a comparison of the flow field between PIV measurements and numerical simulation is carried out. The directions of the flow fields agree very well. Only at the spray edge some vectors disagree. In this region the PIV algorithm cannot distinguish reliably between tracer particles and spray droplets. This will be overcome in further experiments by using fluorescing tracer particles. This enables a separate recording of droplet vectors and gas flow field vectors [5].

Figure 5 shows numerical calculations for the annular orifice injector. Inside the hollow cone a flow field arises which is directed towards the injector tip. The vapor distribution follows the liquid distribution.

4.3. Air entrainment

The amount of entrained air into the spray region essentially affects the vaporization rate. Therefore air entrainment is an important parameter to judge different injection strategies.

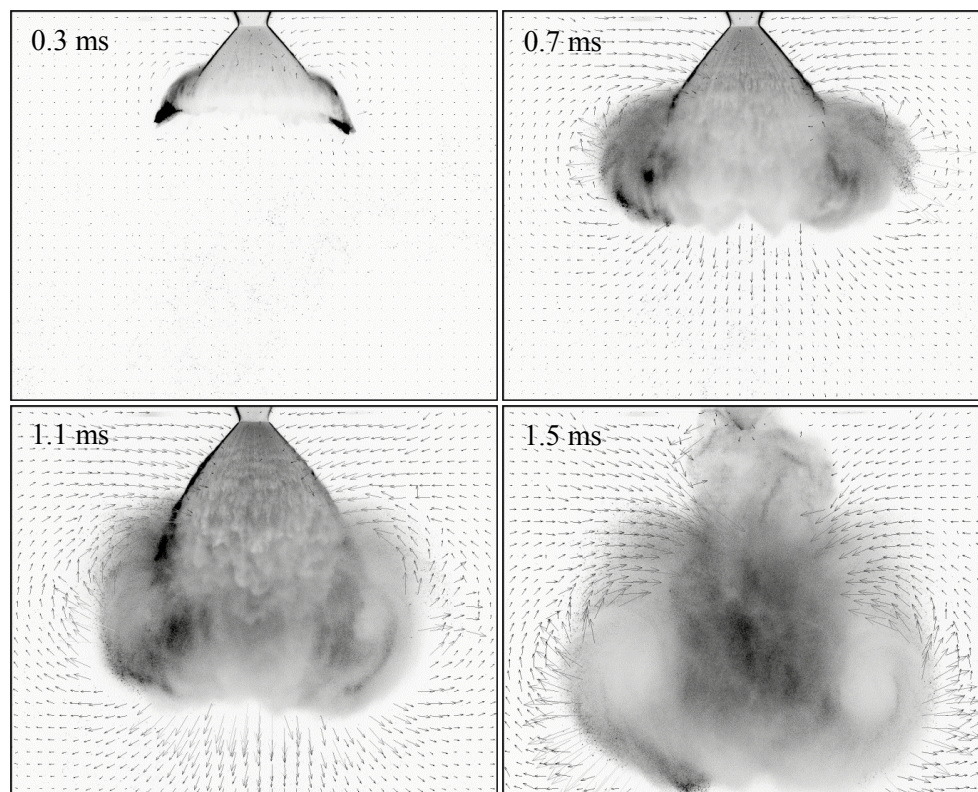


Figure 3: PIV measurements at different time steps, annular orifice spray, injection duration 1.1 ms.

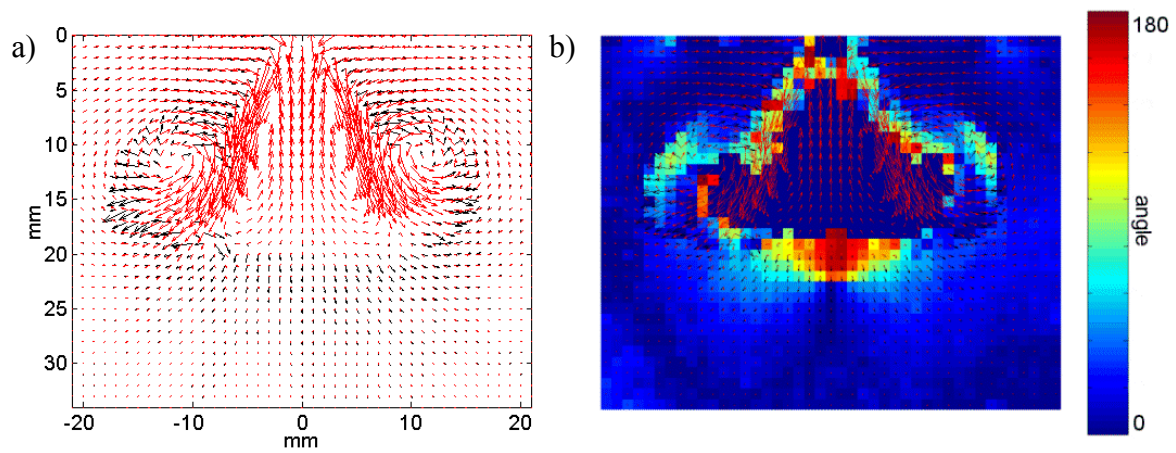


Figure 4: a) Comparison of the gas flow field between PIV (black) and simulation (red) at 0.7 ms, b) difference angles between velocity vectors.

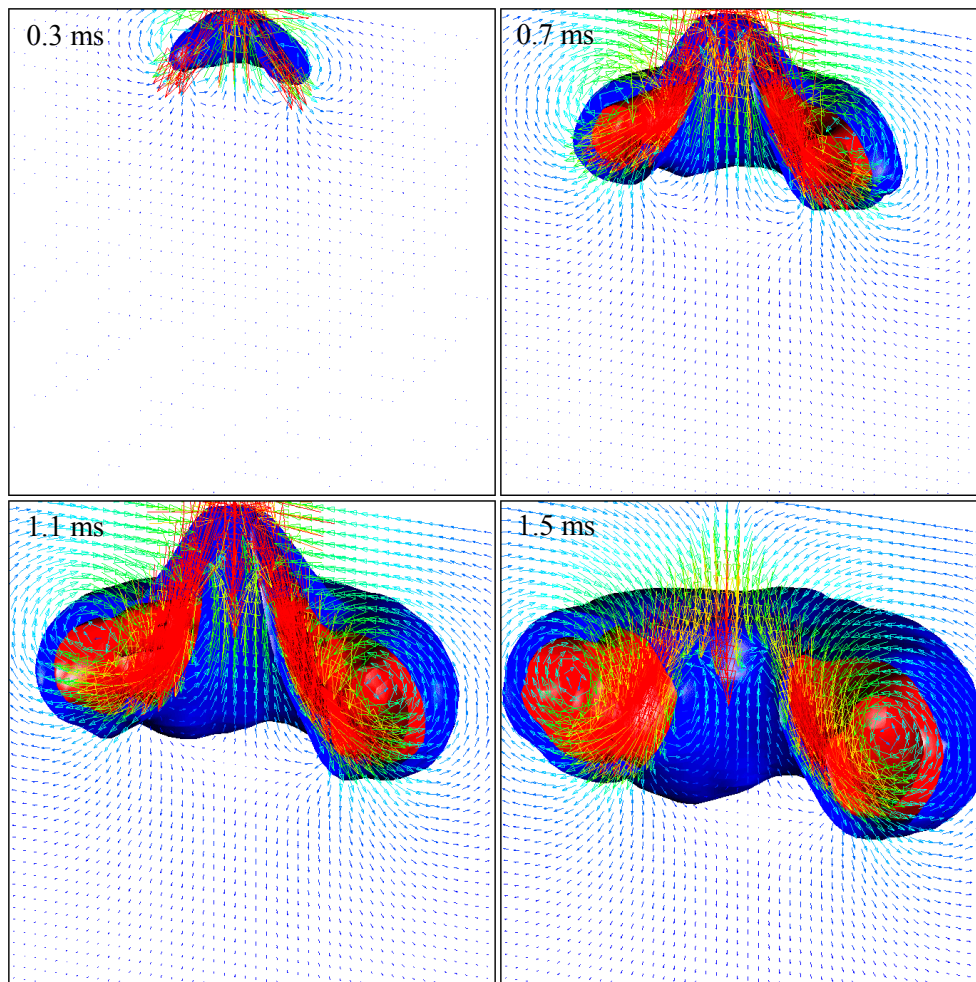


Figure 5: Vapor distribution, visualized by isosurfaces for constant equivalence ratios, and gas flow field from numerical simulation at different time steps, annular orifice injector, injection duration 1.1 ms.

In this work air entrainment is defined as air mass flow through a control surface. Isosurfaces of constant fuel concentrations corresponding to the spray edge are chosen as control surfaces. The mass flow is calculated then regarding the equation

$$\dot{m} = \iint \rho_g \bar{v}_{rel} dS,$$

with the gas density ρ_g , the relative velocity v_{rel} between the gas velocity and the spray velocity and the isosurface S . As from PIV and laser light sheet technique only two dimensional data is available, the isosurface is calculated by rotating the corresponding isoline around the center line of the spray. This approach is justified as the annular orifice spray is an axis symmetrical spray. By calculating isolines for two following time steps, the spray velocity results from the distance of the isolines and the time offset between the time steps. Figure 6 shows the entrainment evaluation based on experimental data. The gas velocities were extracted from PIV measurements on a dummy line slightly away from the isoline to enhance accuracy. Figure 7 shows the calculated entrainment for numerical data. The quantification of the entrainment was done for three spray regions: trailing edge (A), vortex (B) and spray tip (C). The control surfaces for the two approaches differ. For the experimental evaluation the control surface has to cover the whole spray as no flow field information is available in the spray center. In contrast the numerical approach shows the hollow cone structure of the spray. Considering this the differences in the entrainment calculations become obvious. The experimental approach shows the highest entrainment at the spray tip while for the numerical approach a noticeable air entrainment takes place at the vortex. Due to the small surface of the trailing edge the overall entrainment is rather small in this region.

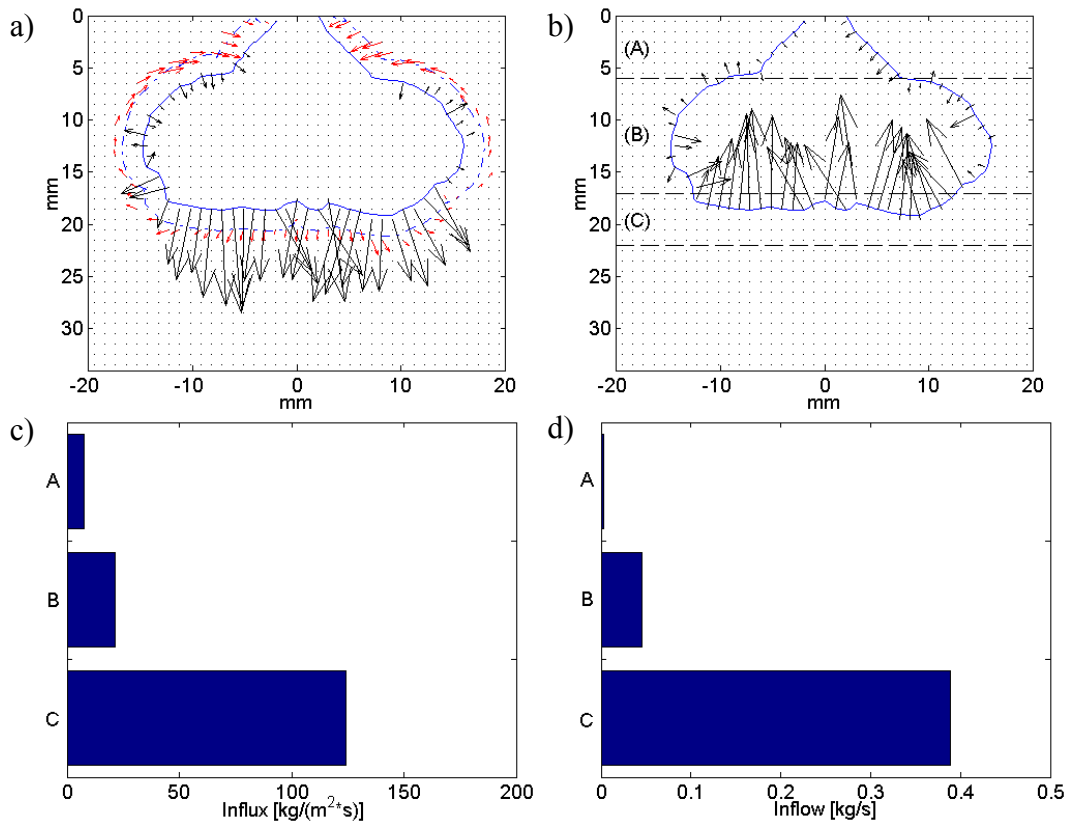


Figure 6: Air entrainment from experimental data. a) Spray (black) and gas velocities (red), b) air entrainment into the spray and quantification of influx (c) and inflow (d) for three spray regions.

A numerical analysis of air entrainment for different ambient pressures and temperatures corresponding to three injection timings, 88° crank angle (CA), 46° CA and 33° CA before top dead center (TDC), has been performed. Figure 8 shows the temporal development of the spray surface area, the relative velocity between spray and gas phase, influx and inflow of air into the spray. The spray with the biggest spray surface area and highest relative velocity with the gas phase develops for the early injection timing ($p_{amb}=2$ bar and $T_{amb}=370$ K) due to the low ambient pressure. But nevertheless the highest air entrainment is found for late injection timing ($p_{amb}=10$ bar and $T_{amb}=572$ K) as the higher air density overcompensates the effects of smaller spray surface and lower relative velocity.

5. Conclusion

The temporal evolution of the liquid distribution and the spray induced air flow were examined for an annular orifice injector using spray tomography and particle image velocimetry. Numerical calculations showed a good agreement with experimental data. They allowed to assess the gas flow field inside the spray and the vapor distribution. It was seen that the induced air flow influences strongly the spray propagation. An approach for the quantification of air entrainment from experimental as well as numerical data was shown. The two approaches differ in the control surfaces used to calculate the entrainment, but both showed a strong air entrainment at the spray head. The variation of injection timing showed the effects of spray surface, relative velocity and air density on air entrainment. A late injection timing turned out to be favorable.

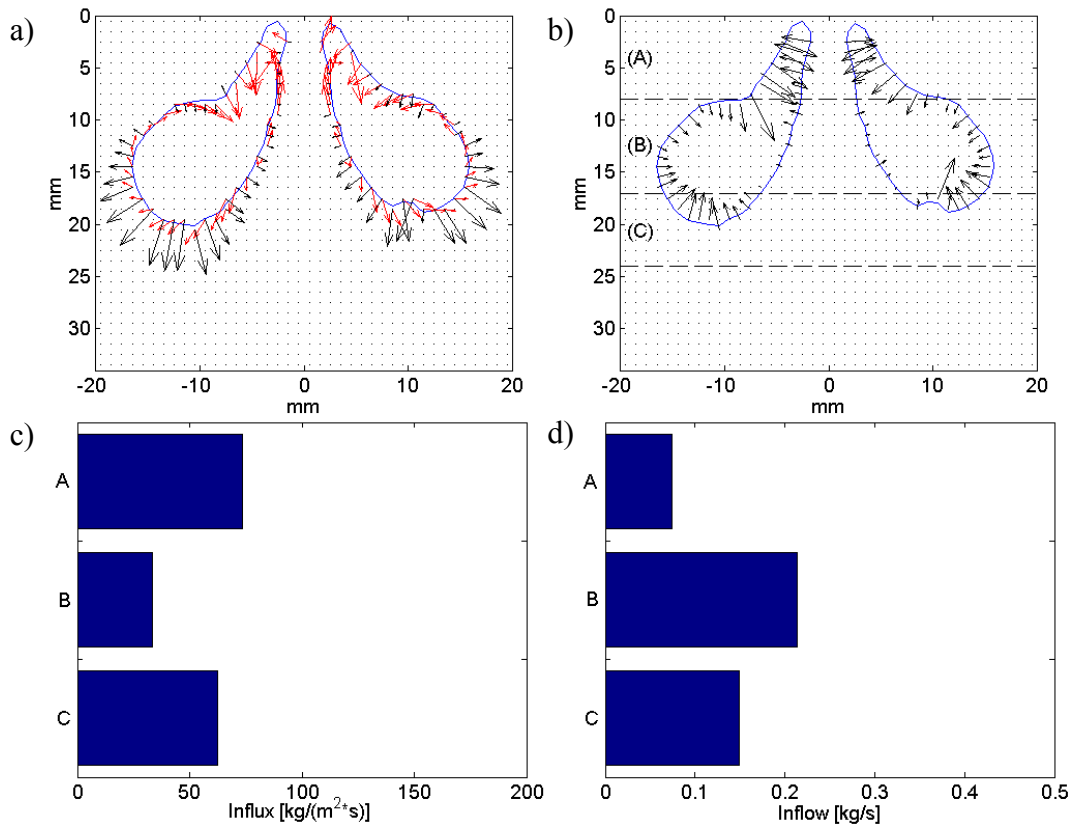


Figure 7: Air entrainment from experimental data. a) Spray (black) and gas velocities (red), b) air entrainment into the spray and quantification of influx (c) and inflow (d) for three spray regions.

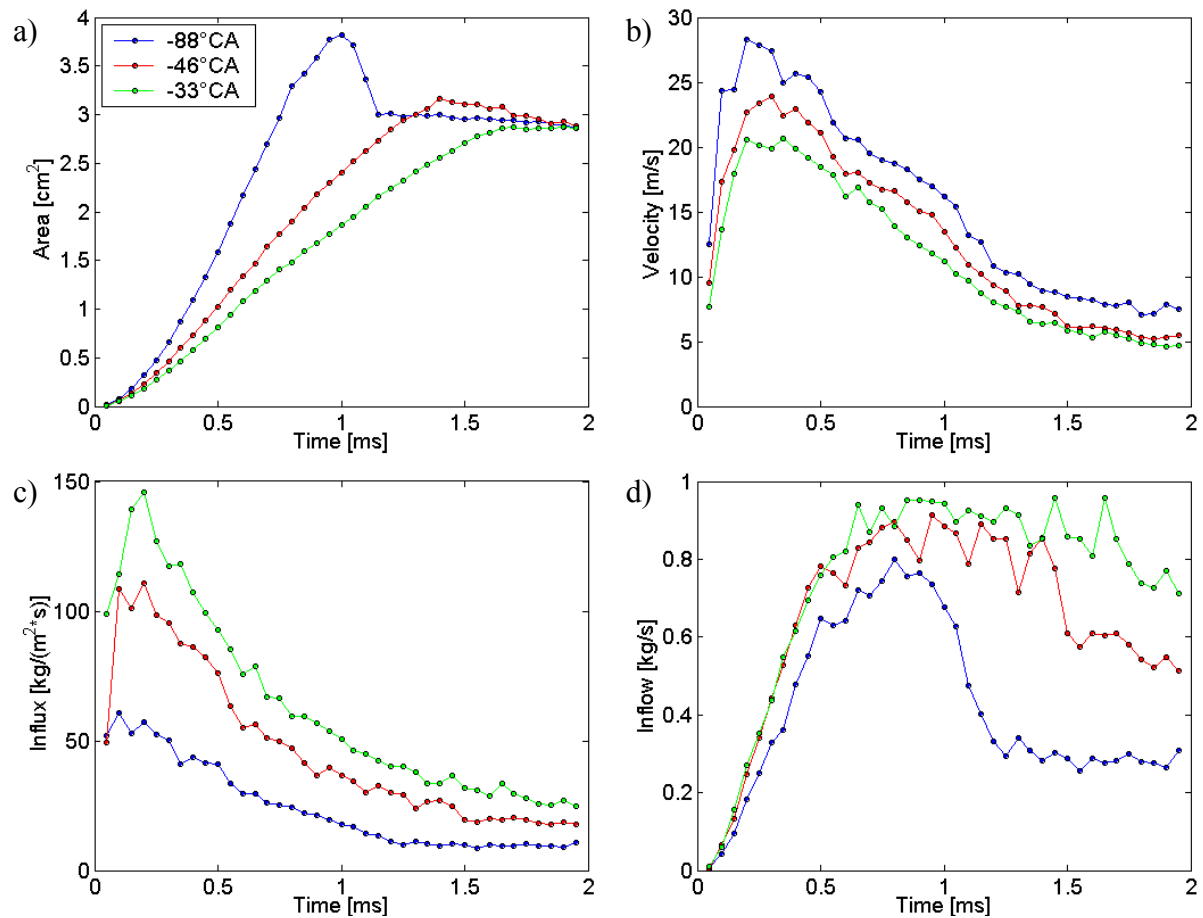


Figure 8: Numerical analysis of air entrainment for different injection timings: 88°CA, 46°CA and 33°CA before TDC. a) Spray surface area, b) relative velocity between spray and gas phase, c) influx and d) inflow into the spray.

6. References

- [1] Ortmann R, Arndt S, Raimann J, Grzeszik R. *Methods and analysis of fuel injection, mixture preparation and charge stratification in different direct injected spark ignited engine*. SAE-Paper, 2001-01-0970, SP-1584; 2001.
- [2] Arndt S, Gartung K and Brüggemann D. *Spray structure of high pressure gasoline injectors: analysis of transient spray propagation and spray-gas momentum transfer*. Proceedings of the 15th ILASS-Europe Conference; 2001 Sep 2-6; Zürich.
- [3] Heinen C. *Weiterentwicklung und Verifizierung der Einsatztauglichkeit neuartiger laseroptischer Tomographieverfahren in der Strömungsmesstechnik*. PhD Thesis, University of Karlsruhe; 2001.
- [4] AVL List GmbH. *FIRE User's Guide Version 7*. AVL List GmbH; 2000.
- [5] Rottenkolber G, Gindele J, Raposo J, Dullenkopf K, Hentschel W, Wittig S, et al. *Spray analysis of a gasoline direct injector by means of two simultaneous two phase PIV*. Proceedings PIV'99; 1999 Sep 16-18; Santa Barbara.